

# Cooperative single-photon subradiant states

H. H. Jen,<sup>1,\*</sup> M.-S. Chang,<sup>2</sup> and Y.-C. Chen<sup>2</sup>

<sup>1</sup>*Institute of Physics, Academia Sinica, Taipei 11529, Taiwan*

<sup>2</sup>*Institute of Atomic and Molecular Sciences, Academia Sinica, Taipei 10617, Taiwan*

(Dated: December 9, 2024)

We propose a set of subradiant states which can be prepared and detected in a one-dimensional optical lattice. We find that the decay rates are highly dependent on the spatial phases we manipulate to imprint on the atomic system, which gives systematic investigations of the subradiance in the fluorescence experiments. The time evolution of these states can have long decay time where hundred milliseconds of lifetime is predicted up to one hundred atoms. They can also show decayed Rabi-like oscillations with a beating frequency determined by the difference of cooperative Lamb shift in the subspace. Experimental requirements are also discussed for practical implementation of the subradiant states. Our proposal provides a novel scheme for quantum storage of photons in arrays of two-level atoms through the preparation and detection of subradiant states, which offer opportunities for quantum information processing in optical lattices.

PACS numbers: 42.50 Gy, 42.50 Ct, 42.50 Dv

**Introduction.** Cooperative light-matter interactions [1] play an important role in the aspects of correlated spontaneous emissions, quantum entanglement [2], and preparation of exotic quantum states [3–7]. Superradiance [8, 9] and associated cooperative Lamb shift (CLS) [10, 11] are examples that demonstrate the collectivity in exchanging photons within an atomic ensemble. Subradiance, on the other hand, is a less aware collective effect complementary to the superradiance, which spontaneously emits light in a rate lower than the natural one. Single-photon superradiance [12–14] and subradiance are of great interests in that the dimensionality of the Hilbert space is restricted to the order of the number of atoms  $N$  only, thus simplifies the dynamical couplings with each other.

Resonant dipole-dipole interaction [15, 16] is regarded to initiate the superradiance with properties of directional emissions in an enhanced spontaneous decay rate. Because of its spatial dependence in the short range ( $\propto 1/r^3$ ) and the long range ( $\propto 1/r$ ), the decay behavior heavily depends on the density and geometry of the interacting medium, and additionally excitation polarizations. Recent experiments demonstrated a shorter timescale of the second-order correlation of two photons in the cascade atomic ensembles [17, 18], and a significant redshift of CLS in various atomic systems including the embedded Fe atoms in the planar cavity [19], an atomic vapor [20], an ionic atomic array [21], and a cold atomic ensemble [22]. Subradiant lifetime was also recently measured in the ring plasmonic nanocavities [23], the ultracold molecules [24], and a cold atomic ensemble [25].

If the excitation field is weak or even a single photon is driving a two-level atomic system ( $|g\rangle$  and  $|e\rangle$  for the ground and excited states respectively), the superradiance and accompanied CLS [11, 26] emerge from the symmetrical and singly-excited state or timed Dicke state [12],

$$|\phi_N\rangle = \frac{1}{\sqrt{N}} \sum_{\mu=1}^N e^{i\mathbf{k}\cdot\mathbf{r}_\mu} |e\rangle_\mu |g\rangle^{\otimes(N-1)}, \quad (1)$$

where  $\mathbf{k}$  is the wavevector of the excitation pulse of a single photon, and the tensor product denotes the rest of  $(N-1)$

ground state atoms other than the one being excited, that is  $|e\rangle_\mu |g\rangle^{\otimes(N-1)} \equiv |\psi_\mu\rangle$ . Since the symmetrical state is approximately decoupled from the rest of  $(N-1)$  orthogonal and nonsymmetrical (NS) states  $\{|\phi_{m\neq N}\rangle\}$ , the emission long after the superradiance (afterglow if there is any because of extremely low probability in the limit of extended medium) suggests the occupation of these states [14]. These NS states responsible of the spontaneous emission in a rate lower than the natural decay one are subradiant states, which were observed in a large cloud of cold atoms [25]. A recent proposal also suggested to preparation and detection of subradiant states in the scheme based on subensembles [27].

A complete Hilbert space for a single photon interacting with the atomic ensemble has been proposed for these normalized NS states [14],

$$|\phi_m\rangle = \sum_{\mu=1}^N \left( C - \frac{\sqrt{N}+1}{N-1} \delta_{\mu N} - \delta_{\mu m} \right) e^{i\mathbf{k}\cdot\mathbf{r}_\mu} |\psi_\mu\rangle, \quad (2)$$

for  $m \in [1, N-1]$  with  $C \equiv (1 + 1/\sqrt{N})/(N-1)$ . An alternative construction of the complete space is proposed in terms of Dicke's states where the formalism of singlet and triplet states in the angular momentum eigenstates provides the foundation to construct the Hilbert space [28],

$$|\phi_m\rangle = \frac{\sum_{\mu=1}^m e^{i\mathbf{k}\cdot\mathbf{r}_\mu} |\psi_\mu\rangle - m e^{i\mathbf{k}\cdot\mathbf{r}_{m+1}} |\psi_{m+1}\rangle}{\sqrt{N(N-1)}}. \quad (3)$$

The difference of the above two NS states is that the first involves all the atoms whereas the second involves a subset of atoms in specific positions. In the perspective of experimental preparation of these NS states, both require exquisite control on the coefficients of each constituent atoms, including the amplitudes and phases, in order to evolve from the initially prepared  $|\phi_N\rangle$  state to the targeted NS states. Similarly in the setting of spatially-separated subensembles [27], intentional preparation of specific subradiant state can be feasible by controlling the phases of each subensembles though it would be more difficult technically for more subensembles.

The issue with these analytic NS states is that they are not the eigenstates of the Hamiltonian, and therefore each NS state cannot be assessed individually in a controllable way. Below we propose a complete space that involves all the atoms collectively and can be deterministically prepared in the one-dimensional (1D) optical lattice (OL) with one atom per site. Moreover they are excited with equal probabilities, which thus simplifies the state preparation.

*De Moivre states.* We exploit De Moivre's formula which is originally used for the  $n$ th root of unity, that is for a complex number  $z$  such that  $z^n = 1$ . To construct the complete  $N$  states for single-photon excitation, we take the roots of  $z^N = 1$  as indication of the state coefficients, which are  $e^{i2\pi m/N}$  for  $m \in [1, N]$ . Another useful identity of the sum of all roots,  $\text{SR}(n) = 0$  for all  $n$  except for  $n = 1$ , indicates the orthogonality of the De Moivre (DM) states we propose in the below. We construct the complete Hilbert space including the symmetrical state  $|\phi_N\rangle$  [29, 30],

$$|\phi_m\rangle = \sum_{\mu=1}^N \frac{e^{i\mathbf{k} \cdot \mathbf{r}_\mu}}{\sqrt{N}} e^{i\frac{2m\pi}{N}(\mu-1)} |\psi_\mu\rangle, \quad (4)$$

where the normalization is ensured, and the orthogonality is  $\langle\phi_m|\phi_n\rangle = \sum_{\mu=1}^N e^{i\frac{2\pi}{N}(\mu-1)(m-n)}/N = \delta_{m,n}$ . The phases of the atomic chain in the 1D OL increase discretely and linearly while the amplitudes of the coefficients are equal in this Hilbert space. The DM states are quite different from the aforementioned NS states where their amplitudes of the coefficients need to be specifically constructed. They also remind us of the discrete Fourier transform that their coefficients are exactly the Fourier series bases since the coefficients  $e^{i2\pi m(\mu-1)/N}$  are  $N$ -periodic. We denote the DM states as cooperative ones in order to study the cooperative spontaneous emissions induced by the long-ranged dipole-dipole interaction, and they can be prepared in a collective way by the external field gradient.

*Experimental realizations.* We propose to use a magnetic field gradient to introduce the linearly increasing phases along the 1D OL shown in Fig. 1. The system can be first prepared in  $|\phi_N\rangle$  by absorbing a single photon. Then the gradient Zeeman field is turned on to evolve  $|\phi_N\rangle$  adiabatically to  $|\phi_{m \neq N}\rangle$ . This evolution can be described by a unitary transformation  $\hat{T} \equiv e^{iV_B\tau_B}$ , where the interaction energy  $V_B = -\mu \cdot \mathbf{B}$ , and  $\tau_B$  is the interaction time. After the evolution the spatial phases of  $V_B\tau_B = m_F g_F \mu_B B \tau_B$  are imprinted on the atoms in the  $m_F$  Zeeman sublevel of the  $F$  hyperfine state. Here  $g_F$  is the Landé  $g$  factor,  $\mu_B$  is the Bohr magneton,  $B'$  is field gradient, and  $z$  represents the positions of the atoms. The measurement of fluorescence afterwards verifies the state we prepare, which therefore provides a systematic study of the super- or sub-radiance of the cooperative single-photon DM states. The subradiant state can be made to store light quanta for much longer time, therefore is potentially useful for quantum memory of light [31].

We use the  $D_2$  transition of  $^{87}\text{Rb}$  atoms as an example, and we choose the ground and excited states as  $|5^2\text{S}_{1/2}, F = 2,$

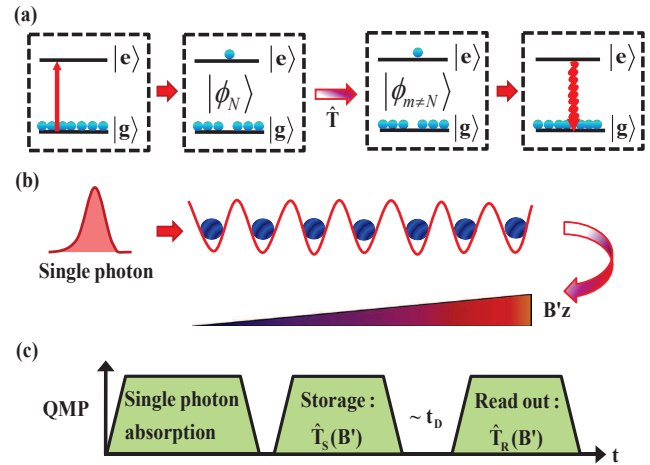


FIG. 1. (Color online) Manipulation of De Moivre states and quantum memory protocol (QMP). (a) Preparation of DM states from the symmetrical  $|\phi_N\rangle$  evolved by a unitary transformation  $\hat{T}$ . (b) Schematic demonstration of single photon absorption by 1D atomic array to form  $|\phi_N\rangle$  followed by a magnetic field gradient to imprint the necessary phases of the DM states. (c) Quantum memory protocol for quantum storage of single photon. After single photon absorption, the system is excited to  $|\phi_N\rangle$  as in (a), and the subradiant state is prepared and evolved from  $|\phi_N\rangle$  by  $\hat{T}_S(B')$  for quantum storage with a time delay  $t_D$ . The storage protocol reads out the photon by  $\hat{T}_R(B') = \hat{T}_S^{-1}(B')$ .

$m_F = -2\rangle$  (denoted as  $|F = 2, m_F = -2\rangle$  with  $g_F = 1/2$ ) and  $|5^2\text{P}_{3/2}, F = 3, m_F = -3\rangle$  (shorthanded  $|F = 3, m_F = -3\rangle$  with  $g_F = 2/3$ ), respectively. The required phase difference for neighboring sites is  $2m\pi/N$  for the  $m$ th DM states, with  $m = 1, 2, \dots, N$ . Thus to access whole Hilbert space of DM states, this phase difference could be as large as  $2\pi$ . Therefore  $B'$  should be as large as  $0.92/(d'_s \tau'_B)$  in unit of  $[\text{mG}/\mu\text{m}]$ , with the dimensionless pulse duration  $\tau'_B$  in milliseconds and the lattice spacing  $d'_s$  in  $\lambda$  which is 780 nm for the  $D_2$  transition. For the order of  $d'_s = 1$  we consider here, the field gradient would be around 92 mG/ $\mu\text{m}$  for 10 microseconds of interaction time, which is within reach of typical experiments. In the perspective of preparing a specific  $m$ th DM state, a longer atomic chain of larger  $N$  also requires a less field gradient or a shorter interaction time to imprint the phase gradients across the whole chain. For example of  $N = 500$  we will demonstrate later, the field gradient just requires 1.8 mG/ $\mu\text{m}$  or the interaction time becomes 200 nanoseconds to prepare  $m = 10$  DM state which still has a reduction of decay rate in the order of  $10^{-2}\Gamma$ . An issue of QMP in Fig. 1(c), however, is the lack of efficiency due to the creation of the superradiant state in the beginning of the DM state preparation, which decays faster than the free space decay rate ( $\sim 26$  ns). To get around this, we can utilize linear Stark shift to imprint the required phases in a rate of MHz to restore the efficiency in QMP.

The technique of position-dependent phase imprinting [32] remind us of controlled reversible inhomogeneous broaden-

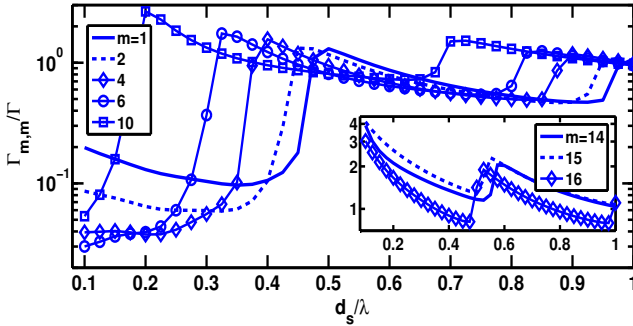


FIG. 2. (Color online) The coupling strengths  $\Gamma_{m,m}$  of the DM states for various lattice spacings with  $N = 16$ . Small coupling strengths appear mostly with  $m \lesssim N/2$  at small lattice spacing  $d_s \approx 0.1 - 0.4\lambda$ , while relatively large ones are demonstrated in the inset near  $m \approx N$ .

ing (CRIB) that is used to implement the quantum memory of light in two-level atoms of praseodymium dopants in yttrium orthosilicate ( $\text{Pr}^{3+}:\text{Y}_2\text{SiO}_5$ ) [33, 34] or warm  $\Lambda$ -type rubidium vapour [35]. On the contrary, we apply the spatial phases to the atoms to manipulate and control the DM states, rather than for the purpose of creating inhomogeneous broadenings on the excited states for efficient absorption of light. Readout process in the proposed protocols is straightforward that the specifically prepared DM states are made to evolve back to  $|\phi_N\rangle$ , which is a superradiant readout.

*Time evolution of DM states.* To investigate what exactly DM states assess the significantly small subradiant eigenvalues and what is the optimal lattice spacing for the lowest eigenvalues, we first study the coupling strength of the resonant dipole-dipole interaction in the DM state bases. Using linear polarization of light propagating along the OL (that is  $\vec{d} \perp \vec{r}_{\mu\nu}$ ), we define the coupling strength as

$$\Gamma_{m,m} = -2\text{Re}\left[\left\langle \phi_m \left| \sum_{\mu,\nu} M_{\mu\nu} \right| \phi_m \right\rangle\right], \quad (5)$$

where  $M_{\mu\nu} \equiv \frac{\Gamma}{2}(-F_{\mu\nu} + i2G_{\mu\nu}\delta_{\nu\neq\mu})$ , and  $F_{\mu\nu}$ ,  $G_{\mu\nu}$  are decay rates and energy shifts from the resonant dipole-dipole interaction between any pair of atoms (see Supplemental Materials [36] for definitions). In Fig. 2 we show the coupling strengths for the DM states, and find that small coupling strengths mostly lie at small lattice spacings less than  $0.4\lambda$ . The period of  $\lambda/2$  in  $d_s$  for the coupling strengths is due to the sinusoidal functions in the dipole-dipole interaction, which is equivalent to a period of  $\pi$ . Similar periodic coupling strengths are demonstrated in infinite atomic lattices with a period of  $2\pi$  [37]. The coupling strengths saturate quickly as  $N$  increases, therefore here we show for the case of  $N = 16$  without loss of generality. Large coupling strengths can be also seen in the inset, showing continuously shifted local peaks from small to large  $m$  states due to equidistant change of  $m$ . From the coupling strength calculations, we later choose specifically  $d_s = 0.1$  and  $0.25\lambda$  that correspond to the lowest

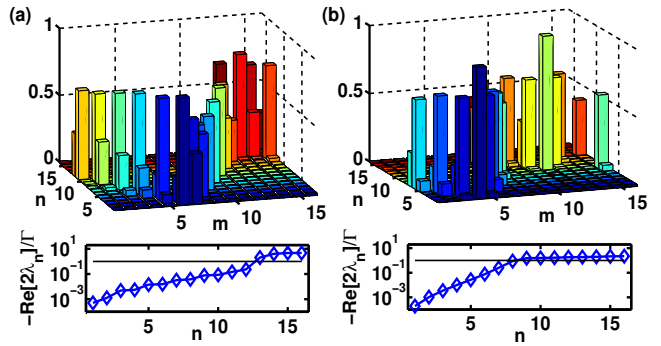


FIG. 3. (Color online) Normalized weightings of DM states  $|\phi_m\rangle$  on the eigenstates  $|\phi'_n\rangle$  for  $N = 16$ . The normalized weightings of DM states show in localized groups of the eigenstates for (a)  $d_s = 0.1\lambda$  and (b)  $0.25\lambda$ . The corresponding ascending order of the real part of the eigenvalues indicates the distribution of the superradiant (above  $\Gamma$ ) and subradiant (below  $\Gamma$ ) decay constants. A horizontal line is used to guide the eye for a natural decay constant which is  $-\text{Re}[2\lambda_n]/\Gamma = 1$ .

coupling strengths for the DM states of  $m = 6$  and  $4$  respectively. These specific DM states will be shown later to demonstrate the smallest decay rate (longest lifetime) respectively.

Next we investigate the time evolution of the DM states which can be observable in the fluorescence experiments. Since the resonant dipole-dipole interaction is long ranged, there is no exact analytical form of the eigenstates in a finite 1D OL. Therefore the DM states we prepare in the 1D OL would couple with several eigenstates that we numerically derived. In Fig. 3 we show the normalized weightings defined in Supplemental Materials [36] for DM states. The weightings demonstrate how significant the eigenvalues  $\lambda_n$  govern the time evolution for the DM states, and they are quite localized in general within two or three eigenstates. This means that the DM states we manipulate to prepare make up an almost closed subspace in the whole eigenbases. For example in (a), we can see that  $m = 2$  and  $11$  form a closed subspace of  $n = 9$  and  $10$  with 98% weightings in the total eigenbases. This reflects that our DM states simulate a decayed Rabi oscillation with a beating frequency of the difference of CLS in the subspace. For a small lattice spacing as  $d_s = 0.1\lambda$ , we clearly see the separated groups of subradiant and superradiant eigenvalues in the ascending order. Specifically for  $d_s = 0.25\lambda$  in (b), more superradiant ones are lying closer to  $\lambda_n = \Gamma/2$  showing less enhanced decay rates due to the larger lattice spacing. For even larger  $d_s$ , we have more eigenvalues distributing near  $\Gamma/2$  as expected for the system approaching the limit of independent atoms.

In Fig. 4, we show the time evolution of the DM state probabilities specifically for  $m = 2$  and  $6$ , and compare with the case of the independent atoms ( $\propto e^{-\Gamma t}$ ). The DM state of  $m = 2$  shows Rabi-like oscillation, which forms a subspace with the DM state of  $m = 11$ . The beating frequency in the plot is estimated as  $0.863\Gamma$ , which has less than 1.2% relative error compared to  $0.853\Gamma$ , the difference of CLS in the subspace of

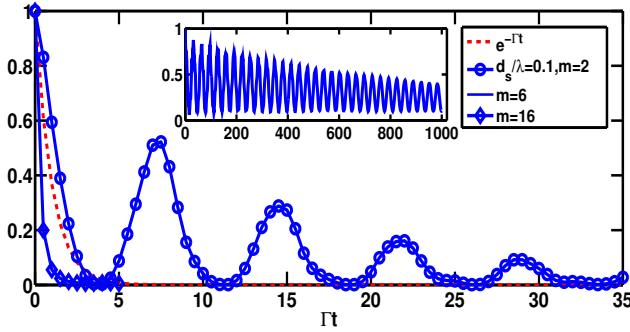


FIG. 4. (Color online) Time evolutions of cooperative single-photon subradiant state probabilities. For  $N = 16$  and  $d_s = 0.1\lambda$ , we demonstrate the time evolutions of DM states of  $m = 2$  ( $\circ$ , oscillatory and subradiant),  $m = 6$  (inset, oscillatory and subradiant), and  $m = 16$  ( $\diamond$ , superradiant), compared to the natural decay one  $e^{-\Gamma t}$  (dash).

$n = 9$  and 10. In this way the DM states provide a systematic measurement of relative CLS from the fluorescence experiments. The symmetric DM state  $|\phi_N\rangle$  with  $m = 16$  shows superradiance as expected, which however involves several superradiant eigenmodes as seen in Fig. 3(a). The most interesting and important observation is for the DM state of  $m = 6$  where we plot the envelopes of the long-time emission intensity. This DM state is mostly comprised of two eigenmodes with the lowest real parts of the two eigenvalues ( $5.1 \times 10^{-4}$  and  $1.3 \times 10^{-3}\Gamma$ ) with 99% weightings among all. To determine the lowest decaying rate of the subradiant DM states, we use an exponential fit of  $e^{-\Gamma_f t}$  to the emission envelopes for different number of atoms and lattice spacings in Fig. 5. We show as low as the order of  $10^{-7}\Gamma$  decay rate for the DM state of 100 atoms, which is equivalent to the lifetime of several hundred milliseconds in the system of two-level atoms. When  $d_s \gtrsim 0.5\lambda$  as shown in the inset, the decay constant barely depends on the atom numbers. The parenthesis shows the specific  $m$ th DM state that occupies the most of the eigenmodes with the lowest real part of the eigenvalue, which scales with atom numbers. The cases of the lattice spacings at 0.5 and 1 $\lambda$  sharing the same DM states again reflects the period of  $\lambda/2$  in the coupling strengths. For even longer 1D chains, the lifetime can be longer and seems to reach indefinitely to the zero decay for  $d_s$  shorter than  $0.4\lambda$ , although it is more challenging for the experiments in the perspectives of stability and controllability. Also the fidelity of preparing the genuine DM states for longer 1D chains would suffer from the unwanted inhomogeneous broadenings by the magnetic field gradient.

Our proposal for the DM states implemented in a 1D OL can potentially be realized in 1D hard core bosons [38, 39], ions [21], color center defects in diamond [40, 41], or atom-fiber system [42]. With a scalable 1D array, decoherence-free regime can be feasible, which adds the richness and robustness to quantum information network. Our setting is also alternative to investigating the many-body long-range interactions in the alkaline-earth-metal atoms [43] and the cooperative behavior in the square and kagome lattices [44]. For prepara-

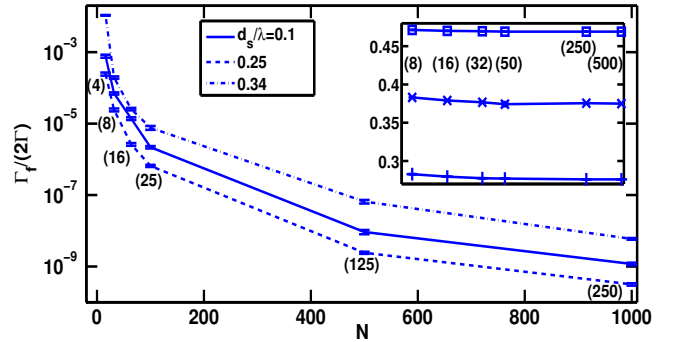


FIG. 5. (Color online) Fitted decay constants. For atom numbers  $N = 16, 32, 64, 100, 500$ , and  $1000$ , we show the fitted lowest decay constant  $\Gamma_f$  in logarithmic scale by the envelope of  $e^{-\Gamma_f t}$  for  $d_s = 0.1$  (solid),  $0.25$  (dash),  $0.34\lambda$  (dash-dot), and for  $d_s = 0.5$  ( $\times$ ),  $0.68$  ( $+$ ), and  $1\lambda$  ( $\square$ ) in the inset where the cases of  $0.5$  and  $1\lambda$  share the same DM states denoted by the parenthesis. The parenthesis ( $m$ ) shows the  $m$ th DM state that demonstrates the lowest  $\Gamma_f$  for the cases of  $d_s = 0.25$  and  $0.5\lambda$  for demonstration. The error bar indicates the deviation for fitted exponential decay constants with or without the intercept of the zero time point.

tion of the single-photon subradiant states, a scheme with Rydberg atomic excitations [45, 46] is sufficient to generate singly-excited cooperative states via dipole blockade effects along with phase imprinting. We expect even richer dynamical couplings between atoms by introducing this additional long-ranged dipole-dipole interactions.

In conclusion, we propose a complete Hilbert space of cooperative single-photon states that can be prepared and manipulated in the two-level atoms in a 1D OL. Specifically these cooperative subradiant states can be systematically studied by varying the spatially-dependent phases we imprint on the atoms by Zeeman field gradient. Cooperative Lamb shift can be also studied in our setting and measured from fluorescence experiments. Hundred milliseconds of lifetime can be observable in several tens of atoms, serving a potentially robust quantum memory of light.

## ACKNOWLEDGEMENTS

This work is supported by the Ministry of Science and Technology, Taiwan, under Grant No. MOST-101-2112-M-001-021-MY3 and MOST-103-2112-M-001-011. We are also grateful for the support of NCTS and the fruitful discussions with S.-Y. Lan.

\* sappyjen@gmail.com

[1] L. Mandel and E. Wolf, *Optical coherence and quantum optics*. (Cambridge University Press, 1995).  
[2] K. Hammerer, A. S. Sørensen, and E. S. Polzik, Quantum interface between light and atomic ensembles. *Rev. Mod. Phys.* **82**, 1041 (2010).

- [3] M. J. Hartmann, F. G. S. L. Brandão, and M P. Plenio, Strongly interacting polaritons in coupled arrays of cavities. *Nat. Phys.* **2**, 849 (2006).
- [4] A. D. Greentree, C. Tahan, J. H. Cole, and L. C. L. Hollenberg, Quantum phase transitions of light. *Nat. Phys.* **2**, 856 (2006).
- [5] M. Lewenstein, A. Sanpera, V. Ahufinger, B. Damski, A. Sen(De), and U. Sen, Ultracold atomic gases in optical lattices: mimicking condensed matter physics and beyond. *Adv. Phys.* **56**, 243 (2007).
- [6] D. E. Chang, V. Gritsev, G. Morigi, V. Vuletić, M. D. Lukin, and E. A. Demler, Crystallization of strongly interacting photons in a nonlinear optical fibre. *Nat. Phys.* **4**, 884 (2008).
- [7] I. M. Georgescu, S. Ashhab, and F. Nori, Quantum simulation. *Rev. Mod. Phys.* **86** 153 (2014).
- [8] R. H. Dicke, Coherence in spontaneous radiation processes, *Phys. Rev.* **93**, 99 (1954).
- [9] M. Gross, and S. Haroche, Superradiance: An essay on the theory of collective spontaneous emission. *Phys. Rep.* **93**, 301 (1982).
- [10] R. Friedberg, S. R. Hartmann, and J. T. Manassah, Frequency shifts in emission and absorption by resonant systems of two-level atoms, *Phys. Rep.* **7**, 101 (1973).
- [11] M. O. Scully, Collective Lamb shift in single photon Dicke superradiance. *Phys. Rev. Lett.* **102**, 143601 (2009).
- [12] M. O. Scully, E. S. Fry, Ooi C. H. Raymond, and K. Wódkiewicz, Directed spontaneous emission from an extended ensemble of N atoms: Timing is everything. *Phys. Rev. Lett.* **96**, 010501 (2006).
- [13] J. H. Eberly, Emission of one photon in an electric dipole transition of one among N atoms. *J. Phys. B: At. Mol. Opt. Phys.* **39**, S599 (2006).
- [14] I. E. Mazets, and G. Kurizki, Multiatom cooperative emission following single-photon absorption: Dicke-state dynamics. *J. Phys. B: At. Mol. Opt. Phys.* **40**, F105 (2007).
- [15] M. J. Stephen, First-order dispersion forces. *J. Chem. Phys.* **40**, 669 (1964).
- [16] R. H. Lehmberg, Radiation from an N-atom system. I. General formalism, *Phys. Rev. A* **2**, 883 (1970).
- [17] T. Chanelière, D. N. Matsukevich, S. D. Jenkins, T. A. B. Kennedy, M. S. Chapman, and A. Kuzmich, Quantum telecommunication based on atomic cascade transitions. *Phys. Rev. Lett.* **96**, 093604 (2006).
- [18] B. Srivathsan, G. K. Gulati, B. Chng, G. Maslennikov, D. Matsukevich, and C. Kurtsiefer, Narrow band source of transform-limited photon pairs via four-wave mixing in a cold atomic ensemble. *Phys. Rev. Lett.* **111**, 123602 (2013).
- [19] R. Röhlsberger, K. Schlage, B. Sahoo, S. Couet, and R. Rüffer, Collective Lamb shift in single-photon superradiance. *Science* **328**, 1248-1251 (2010).
- [20] J. Keaveney, A. Sargsyan, U. Krohn, I. G. Hughes, D. Sarkisyan, and C. S. Adams, Cooperative Lamb shift in an atomic vapor layer of nanometer thickness. *Phys. Rev. Lett.* **108**, 173601 (2012).
- [21] Z. Meir, O. Schwartz, E. Shahmoon, D. Oron, and R. Ozeri, Cooperative Lamb shift in a mesoscopic atomic array. *Phys. Rev. Lett.* **113**, 193002 (2014).
- [22] J. Pellegrino, R. Bourgain, S. Jennewein, Y. R. P. Sortais, A. Browaeys, S. D. Jenkins, and J. Ruostekoski, Observation of suppression of light scattering induced by dipole-dipole interactions in a cold-atom ensemble. *Phys. Rev. Lett.* **113**, 133602 (2014).
- [23] Y. Sonnenaud, N. Verellen, H. Sobhani, G. A.E. Vandenbosch, V. V. Moshchalkov, P. V. Dorpe, P. Nordlander, and S. A. Maier, Experimental realization of subradiant, superradiant, and Fano resonances in ring/disk plasmonic nanocavities. *ACS Nano* **4**, 1664 (2010).
- [24] B. H. McGuyer, M. McDonald, G. Z. Iwata, M. G. Tarallo, W. Skomorowski, R. Moszynski, and T. Zelevinsky, Precise study of asymptotic physics with subradiant ultracold molecules. *Nat. Phys.* **11**, 32 (2015).
- [25] W. Guerin, M. O. Araújo, and R. Kaiser, Subradiance in a large cloud of cold atoms. *Phys. Rev. Lett.* **116**, 083601 (2016).
- [26] H. H. Jen, Superradiant cascade emissions in an atomic ensemble via four-wave mixing. *Ann. of Phys. (N.Y.)* **360**, 556 (2015).
- [27] M. O. Scully, Single photon subradiance: Quantum control of spontaneous emission and ultrafast readout. *Phys. Rev. Lett.* **115**, 243602 (2015).
- [28] A. A. Svidzinsky, J.-T. Chang, and M. O. Scully, Dynamical evolution of correlated spontaneous emission of a single photon from a uniformly excited cloud of N atoms. *Phys. Rev. Lett.* **100**, 160504 (2008).
- [29] P. A. Vetter, L. Wang, D.-W. Wang, and M. O. Scully, Single photon subradiance and superradiance revisited: a group theoretic analysis of subradiant states. *Physica Scripta* **91**, 023007 (2016).
- [30] On preparing this manuscript, we are aware of the relevant construction of the subradiant states [29] based on group theory.
- [31] M. Afzelius, N. Gisin, and H. Riedmatten, Quantum memory for photons. *Physics Today* **68**(12), 42 (2015).
- [32] B. Kraus, W. Tittel, N. Gisin, M. Nilsson, S. Kroll, and J. I. Cirac, Quantum memory for nonstationary light fields based on controlled reversible inhomogeneous broadening. *Phys. Rev. A* **73**, 020302(R) (2006).
- [33] G. Hétet, J. J. Longdell, A. L. Alexander, P. K. Lam, and M. J. Sellars, Electro-optic quantum memory for light using two-level atoms. *Phys. Rev. Lett.* **100**, 023601 (2008).
- [34] M. P. Hedges, J. J. Longdell, Y. Li, and M. J. Sellars, Efficient quantum memory for light. *Nature* **465**, 1052 (2010).
- [35] M. Hosseini, B. M. Sparkes, G. Campbell, P. K. Lam, and B. C. Buchler, High efficiency coherent optical memory with warm rubidium vapour. *Nat. Comm.* **2**:174 (2011).
- [36] Supplemental materials for the derivations of the resonant dipole-dipole interactions and normalized weightings of DM states on the eigenfunctions.
- [37] G. Nienhuis, and F. Schulleri, Spontaneous emission and light scattering by atomic lattice models. *J. Phys. B: At. Mol. Phys.* **20**, 23 (1987).
- [38] B. Paredes, A. Widera, V. Murg, O. Mandel, S. Föling, I. Cirac, G. V. Shlyapnikov, T. W. Hänsch, and I. Bloch, Tonks-Girardeau gas of ultracold atoms in an optical lattice. *Nature* **429**, 227 (2004).
- [39] T. Kinoshita, T. Wenger, and D. S. Weiss, Observation of a one-dimensional Tonks-Girardeau gas. *Science* **305**, 1125 (2004).
- [40] H. Weimer, N. Y. Yao, and M. D. Lukin, Collectively enhanced interactions in solid-state spin qubits. *Phys. Rev. Lett.* **110**, 067601 (2013).
- [41] A. Sipahigil, K. D. Jahnke, L. J. Rogers, T. Teraji, J. Isoya, A. S. Zibrov, F. Jelezko, and M. D. Lukin, Indistinguishable photons from separated silicon-vacancy centers in diamond. *Phys. Rev. Lett.* **113**, 113602 (2014).
- [42] D. E. Chang, L. Jiang, A. V. Gorshkov, and H. J. Kimble, Cavity QED with atomic mirrors. *New J. Phys.* **14**, 063003 (2012).
- [43] B. Olmos, D. Yu, Y. Singh, F. Schreck, K. Bongs, and I. Lesanovsky, Long-range interacting many-body systems with alkaline-earth-metal atoms. *Phys. Rev. Lett.* **110**, 143602 (2013).
- [44] R. J. Bettles, S. A. Gardiner, and C. S. Adams, *Phys. Rev. A* **92**, 063822 (2015).

- [45] M. Saffman, T. G. Walker, and K. Mølmer, Quantum information with Rydberg atoms. *Rev. Mod. Phys.* **82**, 2313 (2010).
- [46] T. Peyronel, O. Firstenberg, Q. Liang, S. Hofferberth, A. V. Gorshkov, T. Pohl, M. D. Lukin, and V. Vuletić, Quantum nonlinear optics with single photons enabled by strongly interacting atoms. *Nature* **488**, 57 (2012).

## SUPPLEMENTAL MATERIALS FOR COOPERATIVE SINGLE-PHOTON SUBRADIANT STATES

### RESONANT DIPOLE-DIPOLE INTERACTION

The theoretical analysis is based on the Hamiltonian ( $V_I$ ) of a quantized radiation field interacting with a two-level atomic ensemble of  $N$  atoms. In interaction picture we have ( $\hbar = 1$ )

$$V_I = - \sum_{\mu=1}^N \sum_{\mathbf{k}, \lambda} g_{\mathbf{k}} (\epsilon_{\mathbf{k}, \lambda} \cdot \hat{d}) \hat{S}_{\mu} [e^{-i(w_{\mathbf{k}} t - \mathbf{k} \cdot \mathbf{r}_{\mu})} \hat{a}_{\mathbf{k}, \lambda} + \text{h.c.}], \quad (6)$$

and the dipole operator is defined as

$$\hat{S}_{\mu} \equiv \hat{\sigma}_{\mu} e^{-i\omega_{eg} t} + \hat{\sigma}_{\mu}^{\dagger} e^{i\omega_{eg} t}, \quad (7)$$

where the lowering operator is  $\hat{\sigma}_{\mu} \equiv |g\rangle_{\mu} \langle e|$  with the transition frequency  $\omega_{eg} = \omega_e - \omega_g$ . The coupling coefficient is  $g_{\mathbf{k}} \equiv \langle g | \hat{d} | e \rangle \mathcal{E}(k)$  where the double matrix element of the dipole moment  $\hat{d}$  is independent of the hyperfine structure, and  $\mathcal{E}(k) = \sqrt{kc/(2\epsilon_0 V)}$  with the quantization volume  $V$ . Photon polarization is  $\epsilon_{\mathbf{k}, \lambda}$ , and the unit direction of the dipole operator is  $\hat{d}$ . The bosonic photon operators satisfy the commutation relation  $[\hat{a}_{\mathbf{k}, \lambda}, \hat{a}_{\mathbf{k}', \lambda'}^{\dagger}] = \delta_{\mathbf{k}, \mathbf{k}'} \delta_{\lambda, \lambda'}$ . We use the dipole approximation for the Hamiltonian, and keep the counter rotating-wave parts to correctly account for the energy shift of the resonant dipole-dipole interaction in the below.

Solving Heisenberg equations of motion from the above Hamiltonian, we derive the effective coupled equations for arbitrary atomic operators  $\hat{Q}$  in a Lindblad form that

$$\begin{aligned} \dot{\hat{Q}} = & i \sum_{\mu \neq \nu}^N \sum_{\nu=1}^N G_{\mu\nu} \left[ \hat{\sigma}_{\mu}^{\dagger} \hat{\sigma}_{\nu}, \hat{Q} \right] \\ & + \sum_{\mu=1}^N \sum_{\nu=1}^N F_{\mu\nu} \left[ \hat{\sigma}_{\mu}^{\dagger} \hat{Q} \hat{\sigma}_{\nu} - \frac{1}{2} \left( \hat{\sigma}_{\mu}^{\dagger} \hat{\sigma}_{\nu} \hat{Q} + \hat{Q} \hat{\sigma}_{\mu}^{\dagger} \hat{\sigma}_{\nu} \right) \right], \end{aligned} \quad (8)$$

where  $F_{\alpha, \beta}$  and  $G_{\alpha, \beta}$  are defined as [16]

$$\begin{aligned} F_{\mu\nu}(\xi) \equiv & \frac{3}{2} \left\{ \left[ 1 - (\hat{d} \cdot \hat{r}_{\mu\nu})^2 \right] \frac{\sin \xi}{\xi} \right. \\ & \left. + \left[ 1 - 3(\hat{d} \cdot \hat{r}_{\mu\nu})^2 \right] \left( \frac{\cos \xi}{\xi^2} - \frac{\sin \xi}{\xi^3} \right) \right\}, \end{aligned} \quad (9)$$

$$\begin{aligned} G_{\mu\nu}(\xi) \equiv & \frac{3}{4} \left\{ - \left[ 1 - (\hat{d} \cdot \hat{r}_{\mu\nu})^2 \right] \frac{\cos \xi}{\xi} \right. \\ & \left. + \left[ 1 - 3(\hat{d} \cdot \hat{r}_{\mu\nu})^2 \right] \left( \frac{\sin \xi}{\xi^2} + \frac{\cos \xi}{\xi^3} \right) \right\}, \end{aligned} \quad (10)$$

where  $\xi = |\mathbf{k}| r_{\mu\nu}$ ,  $r_{\mu\nu} = |\mathbf{r}_{\mu} - \mathbf{r}_{\nu}|$  with the transition wave vector  $|\mathbf{k}|$ . This is the origin of resonant dipole-dipole interaction induced by the common light-matter interaction.  $F_{\mu\nu}$

and  $G_{\mu\nu}$  are spatially-dependent decay rates and cooperative Lamb shifts respectively, where  $F_{\mu\nu}$  approaches 1 as  $\xi \rightarrow 0$  while  $G_{\mu\nu}$  becomes divergent. The divergence means the inaccuracy of the quantum optical treatment in such small scale since the atom's internal structure is not accounted for.

### TIME EVOLUTION OF DE MOIVRE STATES

To investigate the time evolution of De Moivre (DM) states, we turn to the Schrödinger equations projected from the above Lindblad form. First we derive the time evolution of the singly-excited states  $|\psi_{\mu}\rangle$  by projecting the coherence operators  $\hat{Q} = |\psi_{\mu}\rangle \langle g|^{\otimes N}$  on  $|g\rangle^{\otimes N}$ . Define the state of the system in Schrödinger picture as  $|\Psi(t)\rangle = \sum_{\mu=1}^N c_{\mu}(t) |\psi_{\mu}\rangle$ , we have

$$\dot{c}_{\mu}(t) = \sum_{\nu=1}^N M_{\mu\nu} c_{\nu}(t), \quad (11)$$

where  $M_{\mu\nu} \equiv \frac{1}{2} (-F_{\mu\nu} + i2G_{\mu\nu} \delta_{\mu \neq \nu})$ , forming a matrix  $\hat{M}$  involving dynamical couplings between any pair of atoms. Using the similarity transformation, we can diagonalize  $\hat{M}$  with the eigenvalues  $\lambda_l$  and eigenvectors  $\hat{U}$ , such that

$$c_{\mu}(t) = \sum_{\nu, n} U_{\mu n} e^{\lambda_n t} U_{n\nu}^{-1} c_{\nu}(t=0), \quad (12)$$

where  $c_{\nu}(t=0)$  denotes the initial condition of the system. When we prepare the atoms in one of the DM states  $|\phi_m\rangle$ , the state vector  $|\Psi(t)\rangle$  can be expressed as  $\sum_{m'=1}^N d_{m'}(t) |\phi_{m'}\rangle$ , which starts to evolve initially from some DM state, that is  $d_{m'}(t=0) = \delta_{m'm}$ . Using the relation of  $d_m = \sum_{\mu=1}^N c_{\mu} e^{-i\mathbf{k} \cdot \mathbf{r}_{\mu} - i2m\pi(\mu-1)/N} / \sqrt{N}$ , eventually we derive the time evolution of the DM states,

$$d_m(t) = \sum_{n=1}^N v_n(m) e^{\lambda_n t} w_n(m), \quad (13)$$

where

$$v_n(m) \equiv \sum_{\mu=1}^N \frac{e^{-i\mathbf{k} \cdot \mathbf{r}_{\mu} - i2m\pi(\mu-1)/N}}{\sqrt{N}} U_{\mu n}, \quad (14)$$

$$w_n(m) \equiv \sum_{\nu=1}^N U_{n\nu}^{-1} \frac{e^{i\mathbf{k} \cdot \mathbf{r}_{\nu} + i2m\pi(\nu-1)/N}}{\sqrt{N}}. \quad (15)$$

We note that  $v_n(m)$  is the inner product of  $m$ th DM state and  $n$ th eigenvector in  $\hat{U}$ , in which  $|v_n(m)|^2$  shows how close DM states are to the eigen ones. We also define a normalized weighting of  $|v_n(m)w_n(m)|^2$  to describe the portion of specific  $\lambda_n$  that governs the time evolution of the DM states.